

## TENSILE AND ELECTRICAL PROPERTIES OF UNIRRADIATED AND IRRADIATED HYCON 3HP™ CuNiBe - S.J. Zinkle and W.S. Eatherly (Oak Ridge National Laboratory)

### OBJECTIVE

The objective of this report is to summarize recent tensile and electrical resistivity measurements on a commercial high-strength, high-conductivity CuNiBe alloy that is being considered for the divertor structure in ITER.

### SUMMARY

The unirradiated tensile properties of two different heats of Hycon 3HP™ CuNiBe (HT Temper) have been measured over the temperature range of 20-500°C for longitudinal and long transverse orientations. The room temperature electrical conductivity has also been measured for both heats. Both heats exhibited a very good combination of strength and conductivity at room temperature. The strength remained relatively high at all test temperatures, with a yield strength of 420-520 MPa at 500°C. However, low levels of ductility (<5% uniform elongation) were observed at test temperatures above 200-250°C, due to flow localization adjacent to grain boundaries. Fission neutron irradiation to a dose of ~0.7 dpa at temperatures between 100 and 240°C produced a slight increase in strength and a significant decrease in ductility. The measured tensile elongation increased with increasing irradiation temperature, with a uniform elongation of ~3.3% observed at 240°C. The electrical conductivity decreased slightly following irradiation, due to the presence of defect clusters and Ni, Zn, Co transmutation products. The data indicate that CuNiBe alloys have irradiated tensile and electrical properties comparable or superior to CuCrZr and oxide dispersion strengthened copper at temperatures <250°C, and may be suitable for certain fusion energy structural applications.

### PROGRESS AND STATUS

#### Introduction

High-strength, high-conductivity copper alloys are being considered for first wall heat sink and divertor structural applications in fusion energy systems such as the proposed International Thermonuclear Experimental Reactor (ITER) [1,2]. The divertor structure poses a particularly challenging operating environment, where good mechanical properties (strength, fatigue, etc.) and high thermal conductivity are required. The proposed operating temperatures for the divertor structure are ~100 to 350°C. The main radiation effects which occur in copper alloys in this temperature regime are radiation hardening (with accompanying embrittlement) and void swelling. Due to the low anticipated damage levels in the ITER divertor structure (<1 dpa), void swelling is not considered to be a design-limiting factor. However, radiation hardening becomes significant in copper alloys at damage levels as low as 0.01 dpa in this temperature range. The uniform elongation of irradiated CuCrZr and alumina-dispersion-strengthened copper (GlidCop) alloys has been found to be <0.5% after neutron irradiation to damage levels of 0.01 to 0.1 dpa at temperatures below 200°C [1-5]. The irradiated tensile elongations of these alloys generally increases above 1% for irradiation temperatures >200°C. However, the strength of these alloys decreases steadily with increasing test temperature and is typically only ~250-300 MPa at a test temperature of 300°C.

Hycon 3HP™ CuNiBe has a superior unirradiated room temperature strength and thermal stress figure of merit compared to other candidate copper alloys [1,6,7]. The room temperature yield strength and electrical conductivity of large (600-1900 kg) heats of Hycon CuNiBe has been measured to be 630-725 MPa and 68-74% IACS [6]. However, there is no known information on the elevated temperature (>200°C) properties of this alloy [1,7] and also relatively little information is available regarding the effects of neutron irradiation on the mechanical and physical properties [1,2]. Recent unpublished work by Singh and coworkers [8] on a European heat of CuNiBe suggested that the irradiated ductility was slightly better than CuCrZr and GlidCop at an irradiation temperature of ~47°C, but significantly worse than these alloys at 250-350°C.

Table 1. Chemical composition (wt.%) of the two heats of Hycon 3HP™ CuNiBe (balance copper).

Heat No.	Ni	Be	Fe	Co	Si	Al	Zn	Sn	Cr	Pb
33667	2.04	0.340	0.020	0.010	0.010	<0.010	<0.010	<0.005	<0.005	<0.003
46546	1.92	0.350	<0.010	<0.010	<0.010	<0.010	<0.010	<0.005	<0.005	<0.003

### Experimental Procedure

Plates of dimensions ~15 x 15 x 2.5 cm were cut from larger plates of two different Hycon 3HP™ CuNiBe heats by Brush-Wellman and shipped to ORNL. Table 1 summarizes the chemical analysis certified by the manufacturer for these two alloy heats. Both heats were received in HT temper (cold-worked and aged) conditions. The general thermomechanical processing steps are summarized elsewhere [9,10]. Heat #46546 was aged to maximize the conductivity. The room temperature yield strength and electrical conductivity quoted by Brush-Wellman ranged from  $\sigma_y=723$  MPa and  $\sigma_e=68\%$  IACS for heat #33667 to  $\sigma_y=633$  MPa and  $\sigma_e=74\%$  IACS for heat #46546. Miniature SS-3 sheet tensile specimens with nominal gage dimensions 0.76 mm x 1.5 mm x 7.6 mm were electro-discharge machined in the longitudinal and long transverse orientations from both heats.

The tensile properties of the SS-3 sheet tensile specimens were determined at 20,100,200,300,400 and 500°C at a crosshead speed of 0.0085 mm/s, which corresponds to an initial strain rate of  $1.1 \times 10^{-3}$ /s in the gage region. The room temperature tests were performed in air, and the elevated temperature tests were performed in vacuum ( $10^{-6}$  to  $10^{-5}$  torr). The specimens were held at the test temperature for 0.5 h prior to the start of each tensile test. One or two specimens were typically tested for each experimental condition. The tensile tests on the neutron irradiated samples were performed on one specimen at each of three irradiation temperatures.

The fracture surfaces of the unirradiated broken tensile specimens were examined using a Hitachi 4100 scanning electron microscope (SEM) equipped with a field emission gun. The detailed microstructure of the unirradiated alloys was examined using a Philips CM12 transmission electron microscope (TEM) operating at 120 kV. TEM specimens cut from as-supplied material and deformed gage regions of selected broken tensile specimens were prepared in a Tenupol jetpolishing apparatus with a solution of 90% orthophosphoric acid in water, cooled to ~0°C.

Four-point probe electrical resistivity measurements were performed following the general recommendations summarized in ASTM Standard Method of Test for Resistivity of Electrical Conductor Materials, ASTM B193-87 (reapproved 1992). Measurements were made on SS-3 sheet tensile specimens at room temperature prior to tensile testing, with a distance between the spring-loaded voltage contacts of 7.10 mm. The temperature was recorded for each measurement and the resistivity data were corrected to a reference temperature of 20°C using the copper temperature coefficient for resistivity of  $dp/dT = 6.7 \times 10^{-11} \Omega\text{-m/K}$ . The typical measured resistance drop was  $\Delta R \sim 150 \mu\Omega$  (ASTM B193-87 recommends  $\Delta R > 10 \mu\Omega$ ). The 100 mA current was supplied by a Keithley 237 Source Measure Unit, and the voltage drop was measured with a Keithley 182 Sensitive Digital Voltmeter equipped with a low thermal connector cable (resolution limit of 1 nV). Thermal emf offset potentials were subtracted using the "relative reading" offset function on the Keithley 182. Ohmic behavior was verified on several specimens by varying the applied current between 10 and 100 mA and measuring the corresponding voltage drop. The typical scatter in the data due to thermal drift was  $\pm 40$  nV. The main source of experimental error was associated with uncertainties in the cross-sectional area of the specimen. The specimen thickness and width were measured to a nominal accuracy of  $\pm 1 \mu\text{m}$  in two different gage locations with a Mitutoyo precision digital micrometer in order to convert the resistance measurements to resistivity values. Nonuniformities in the width and thickness in the specimen gage region caused the typical experimental uncertainty of individual resistivity measurements to be  $\pm 0.5\%$ . A minimum of two different unirradiated specimens were tested for each experimental condition, whereas only one specimen was available for each of the three irradiation temperatures.

Three longitudinal SS-3 tensile specimens machined from heat #46546 were irradiated for 545 h in a core thimble position of the High Flux Beam Reactor (HFBR) at Brookhaven National Laboratory as part of the V1 and V2 irradiation capsules [11]. The irradiation produced to a fast ( $E > 0.1$  MeV) neutron fluence of  $8.3 \times 10^{24}$  n/m<sup>2</sup>, which corresponds to a damage level of  $\sim 0.7$  dpa in copper. The thermal neutron fluence was  $\sim 3 \times 10^{24}$  n/m<sup>2</sup>, which is calculated to produce  $\sim 0.06$  at% Ni and Zn from transmutation reactions with the copper matrix (ignoring additional solute production from resonance and fast neutron reactions). The specimens were contained in three gas-gapped subcapsules which operated at irradiation temperatures of 110, 205 and 240°C. The irradiation temperature was continuously monitored by thermocouples in each subcapsule. Further details regarding the irradiation conditions are given elsewhere [11]. Following irradiation, room temperature Vickers microhardness measurements were performed in the grip region of the specimens and the room temperature electrical resistivity was measured. The specimens were then tensile tested at the irradiation temperature.

## Results

The room temperature (20°C) electrical resistivity of Hycon 3HP™ heat #33667 was measured to be  $26.27 \pm 0.11$  nΩ-m (65.6% IACS). The corresponding resistivity of heat #46546 was  $24.05 \pm 0.06$  nΩ-m (71.7% IACS). No significant orientation dependence was observed for the transverse and longitudinal directions in either heat. The measured conductivities were slightly lower than the values reported by Brush-Wellman of 68% IACS for heat #33667 and 74% IACS for heat #46546.

Figures 1 and 2 summarize the temperature-dependent tensile properties measured for the longitudinal and transverse orientations of both heats of Hycon 3HP™ CuNiBe. The measured yield strengths at room temperature were in good agreement with the values obtained by Brush-Wellman for both heats. The transverse and longitudinal tensile properties were identical for the lower-strength heat (#46546). On the other hand, the yield and ultimate strengths were typically about 40 MPa higher in the longitudinal orientation compared to the long transverse orientation at temperatures above room temperature for heat #33667. Both heats showed very good retention of their strength up to a test temperature of 500°C. For example, the yield strength of heat 33667 in the longitudinal orientation was  $\sim 710$  MPa at 200°C,  $\sim 590$  MPa at 400°C and  $\sim 510$  MPa at 500°C. These strengths are much higher than that obtainable with as-wrought GlidCop Al25 oxide dispersion strengthened copper (335 MPa at 200°C and 256 MPa at 400°C) [1].

The ductility of both Hycon 3HP™ heats decreased rapidly with increasing test temperature. The ductility at room temperature was good ( $e_u \sim 6$  to 9%,  $e_{tot} \sim 10$  to 14%), but the total elongation of both heats dropped to  $\sim 4$  to 5% at 300°C. The uniform elongation of both heats was only about 1% at 400°C, and was only about 0.5% at 500°C. The total elongation decreased to similar values at both of these temperatures. All of the specimens at 400 and 500°C failed at the maximum load, without any macroscopic necking (although there was some work hardening prior to failure). The shape of the elevated temperature stress-strain curves suggested that the poor ductility may be associated with flow localization (similar to the tensile behavior of copper alloys irradiated at low temperatures).

The fracture surfaces of several specimens were examined with scanning electron microscopy in order to investigate the cause of the poor ductility at elevated temperatures. Figure 3 compares the fracture surfaces of specimens tensile tested at room temperature and 500°C. The room temperature failure mode was ductile transgranular fracture, whereas the failure mode at 400 and 500°C was ductile intergranular fracture. The fracture surface of a specimen tensile tested at 300°C exhibited predominantly dimpled transgranular fracture, with  $\sim 25\%$  of the fracture surface showing ductile intergranular fracture. As evident in Fig. 3, the fracture surfaces at 500°C and room temperature appeared identical at high magnification (typical dimple size of a few microns), even though the deformation mode changes from intergranular to transgranular. This suggests that the loss of macroscopic ductility at elevated temperatures is due to localized deformation at the grain boundaries, due to their relatively weak strength compared to the grain interior.

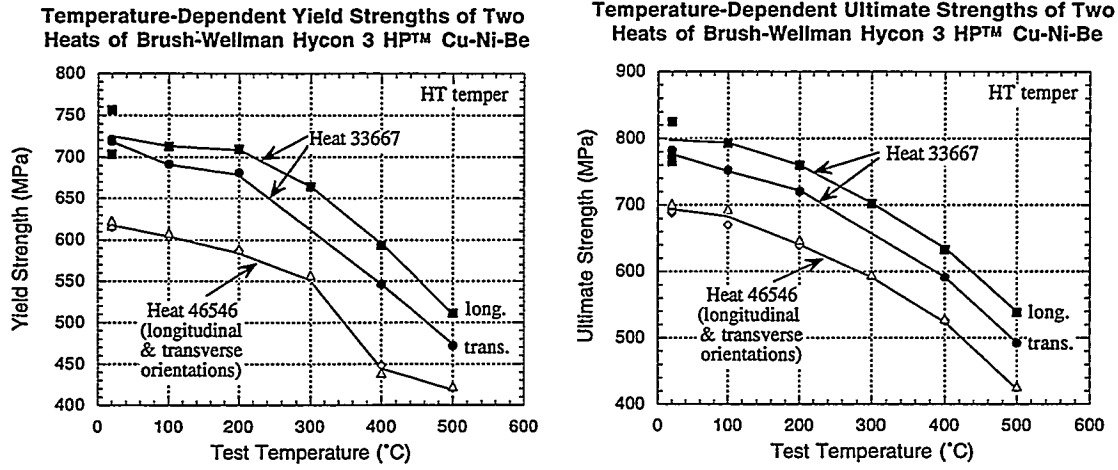


Fig. 1. Summary of the temperature-dependent yield and ultimate strengths of two different heats of Hycon 3HP<sup>TM</sup> CuNiBe (HT temper).

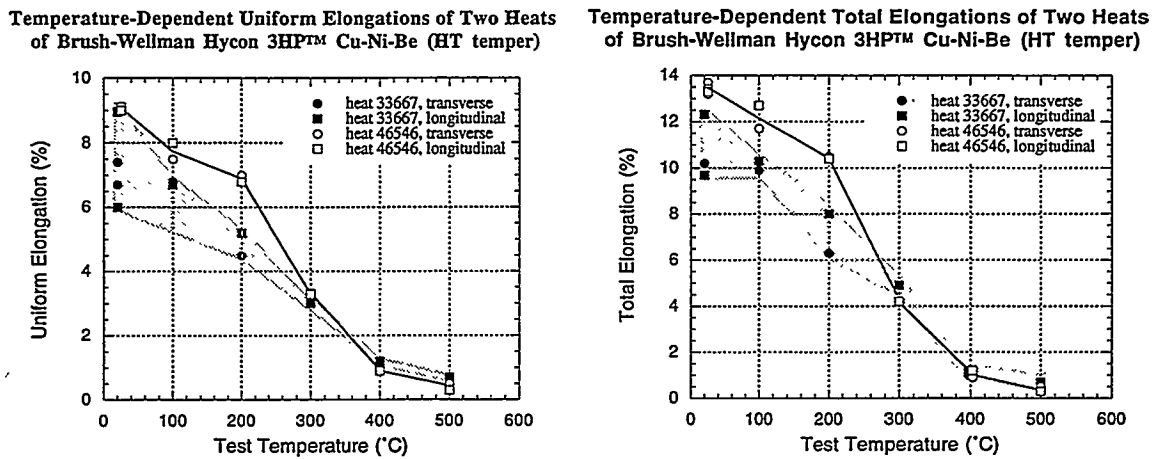


Fig. 2. Summary of the temperature-dependent uniform and total elongations of two different heats of Hycon 3HP<sup>TM</sup> CuNiBe (HT temper).

ORNL-PHOTO 4119-96

FRACTURE SURFACES OF HYCON 3HP™ CuNiBe  
FOLLOWING TENSILE TESTING AT 20 AND 500°C

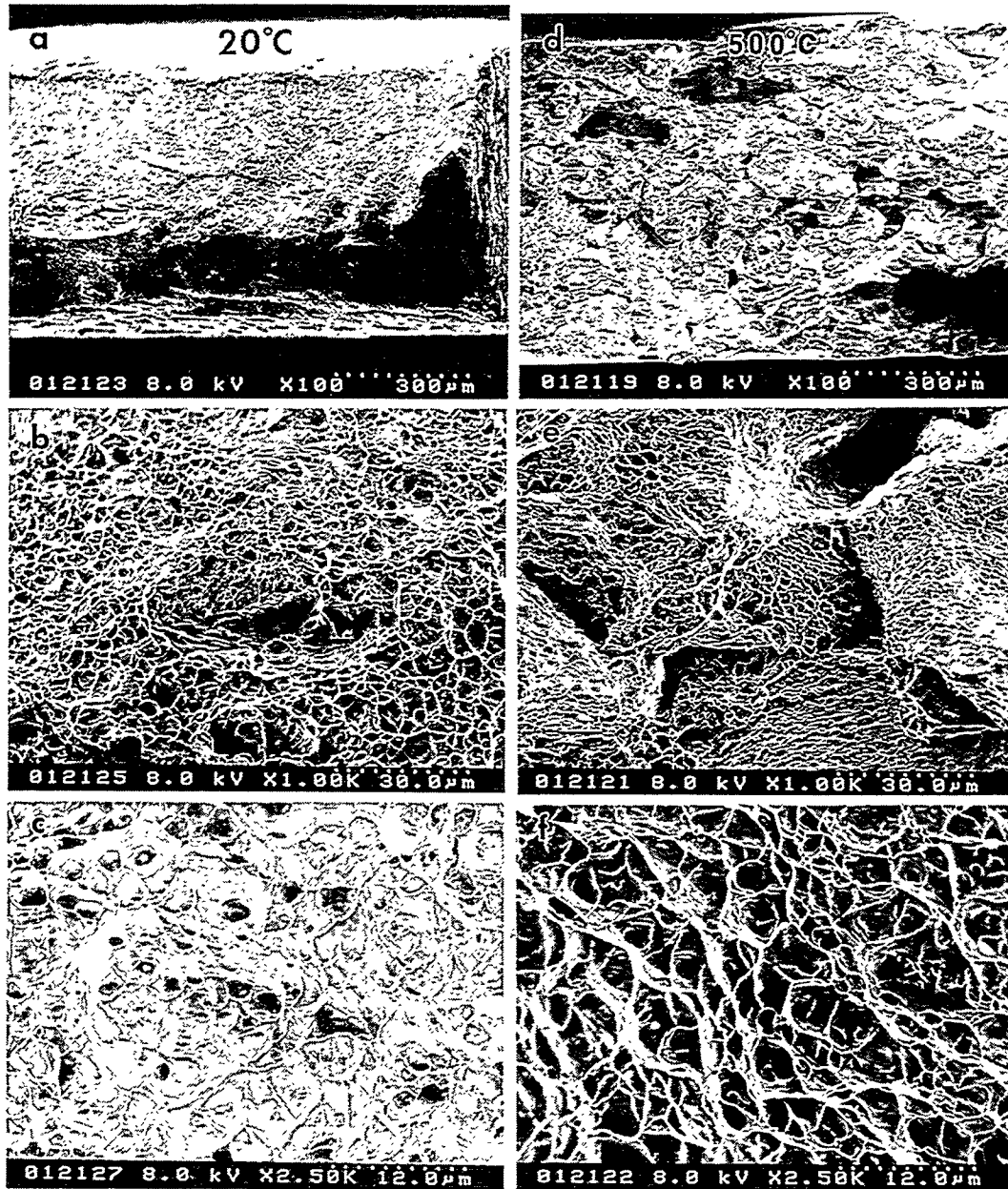


Fig. 3. Fracture surfaces of unirradiated Hycon 3HP™ CuNiBe heat #46546 (longitudinal orientation) following tensile testing at room temperature (a-c) and 500°C (d-f).

A preliminary analysis of the Hycon 3HP™ CuNiBe microstructure by transmission electron microscopy revealed the presence of three types of precipitates. As shown in Fig. 4, a low density ( $\sim 1$  to  $5 \times 10^{17}/\text{m}^3$ ) of large precipitates with a typical diameter of 1 to 5  $\mu\text{m}$  were visible at low magnifications. These large particles were present in both nondeformed and tensile-tested specimens, and are likely sites for microvoid initiation during the tensile testing. Previous work by Guha [12] identified these large particles as an intermetallic beryllide with a cubic B2 structure and a lattice parameter of 0.279 nm. The second type of precipitate was located along grain boundaries, and had a typical size of  $\sim 50$  nm. Several of these grain boundary precipitates are arrowed in Fig. 5. These precipitates were reported to be Ni-rich by Spitznagel et al. [13]. The third type of precipitate occurred uniformly throughout the matrix (Figs. 5 and 6), and is responsible for the high strength of this alloy. Initial measurements indicate that these semicoherent precipitates have a typical diameter of 15-20 nm and a number density of nearly  $1 \times 10^{24}/\text{m}^3$ . Previous studies on CuNiBe alloys have identified these semicoherent precipitates as either GP zones [13] or a mixture of GP zones and  $\gamma''$  phase [12]. In the present study, electron diffraction patterns showed streaks along  $\langle 001 \rangle$  directions which were bunched into intensity maxima at  $\pm 2/3(002)$  positions. According to the Cu-Be precipitation sequence reviewed by Rioja and Laughlin [14], this indicates that these matrix precipitates are predominantly  $\gamma''$  phase.

A small ( $\sim 20$  nm width) precipitate-free zone was observed near the grain boundaries in nondeformed and tensile-tested specimens. The width of the precipitate-free zone did not increase following tensile testing at  $500^\circ\text{C}$ , where low macroscopic ductility was observed in the tensile tests. Figure 7 shows an example of the microstructure of the deformed gage region of a tensile specimens tested at  $500^\circ\text{C}$ . A twin boundary is imaged in this micrograph, and the zone axis is near  $[110]$  in both grains.

Tables 2 and 3 summarize the electrical resistivity, Vickers microhardness, and tensile data obtained on the three SS3 tensile specimens of CuNiBe heat #46546 (longitudinal orientation) following HFBR neutron irradiation to  $\sim 0.7$  dpa. The Vickers microhardness measurements were performed at room temperature at a load of 1 kg and had a standard error of  $\pm 1$  VHN. The tensile measurements were obtained at a test temperature close to the irradiation temperature. Irradiation at  $110^\circ\text{C}$  produced a modest ( $\sim 5\%$ ) increase in the Vickers hardness and ultimate tensile strength of the alloy. The corresponding increase in yield strength and electrical resistivity was  $\sim 15\%$ . A pronounced reduction in uniform elongation occurred for this irradiation temperature. The increment of radiation hardening decreased with increasing irradiation temperature, and amounted to only about a 1% increase in hardness and ultimate tensile strength at  $240^\circ\text{C}$ . This produced a corresponding increase in the tensile ductility with increasing irradiation temperature. Figure 8 shows the tensile load-elongation curves for specimens irradiated at 110 and  $240^\circ\text{C}$ .

The observed increase in electrical resistivity of the 3 specimens following neutron irradiation is in accordance with the expected changes associated with solute transmutation (predominantly Ni, Zn and Co) and defect cluster formation [1,2,4]. The defect cluster density decreases with increasing irradiation temperature above  $\sim 150^\circ\text{C}$ , due to thermal annealing of the vacancy clusters produced in the displacement cascades [1,2]. This factor along with increased solute segregation at the higher irradiation temperatures are likely explanations for the observed decrease in electrical resistivity with increasing irradiation temperature. Similar temperature-dependent effects have been observed in neutron-irradiated CuCrZr and GlidCop AL25 alloys [1,2,4].

ORNL-PHOTO 4121-96

## LARGE PRECIPITATES IN HYCON 3HP™ CuNiBe



Fig. 4. Low magnification microstructure of Hycon 3HP™ CuNiBe heat #46546 showing large precipitates in the matrix.

ORNL-PHOTO 4122-96

## PRECIPITATE FORMATION ADJACENT TO A GRAIN BOUNDARY IN HYCON 3HP™ CuNiBe



Fig. 5. Matrix and grain boundary precipitates in CuNiBe heat #46546.

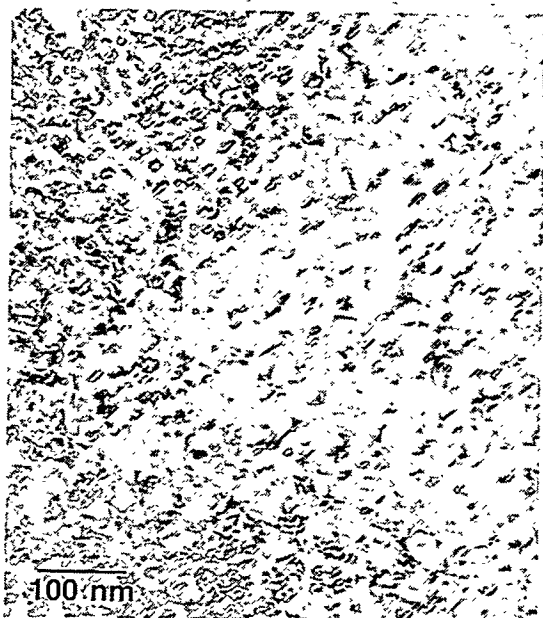


Fig. 6. Semicoherent  $\gamma''$  matrix precipitates in CuNiBe heat #46546.

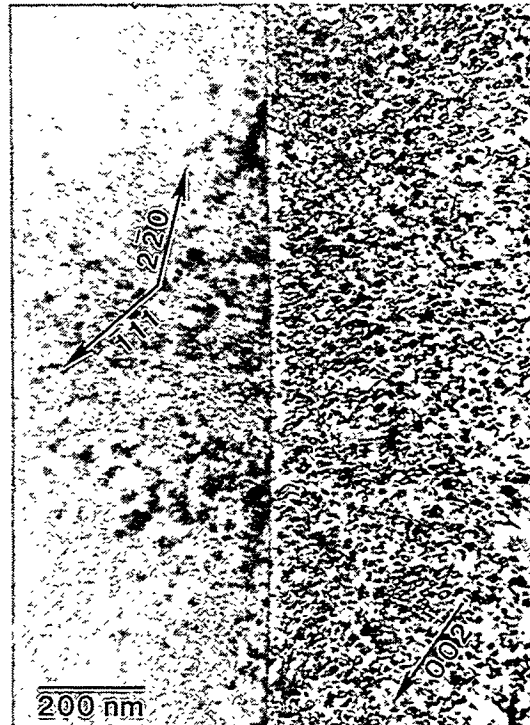


Fig. 7. Microstructure of the deformed gage region of CuNiBe heat #46546 (longitudinal orientation) following tensile testing at 500°C.

Table 2. Summary of electrical resistivity measurements on CuNiBe Hycon 3HP™ heat number 46546, longitudinal orientation.

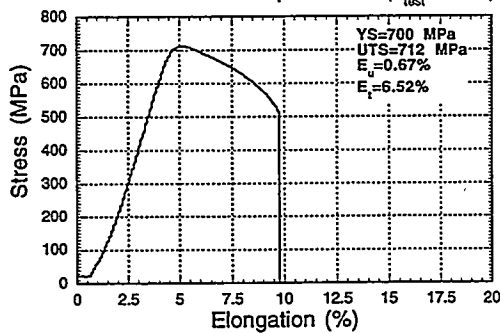
Sample	Condition	$\rho_{20^\circ\text{C}}$ (n $\Omega$ -m)	$\Delta\rho$ (n $\Omega$ -m)	% IACS*	$\Delta\rho/\rho_0$ (%)
CV31,34,18	unirradiated	24.05	—	71.7	—
CV03	110°C, 0.7 dpa	27.71	3.66	62.2	15
CV01	207°C, 0.7 dpa	26.61	2.56	64.8	11
CV02	237°C, 0.7 dpa	25.48	1.43	67.7	6

\*100% IACS = 17.241 n $\Omega$ -m

Table 3. Summary of Vickers hardness and tensile measurements on CuNiBe heat #46546, longitudinal orientation.

Irr. Temp.	Vickers hardness	$\sigma_Y$ (MPa)	$\sigma_{UTS}$ (MPa)	$\epsilon_u$ (%)	$\epsilon_{tot}$ (%)
unirr.	218.5	see Fig. 1	see Fig. 1	see Fig. 2	see Fig. 2
110°C	233.0	700	712	0.67	6.5
207°C	229.0	645	668	0.90	6.7
237°C	219.9	595	633	3.3	6.1

Engineering Stress-Strain Curve for CuNiBe Hycon 3HP Irradiated in HFBR to 0.7 dpa at 110°C ( $T_{test}=110^\circ\text{C}$ )



Engineering Stress-Strain Curve for CuNiBe Hycon 3HP Irradiated in HFBR to 0.7 dpa at 237°C ( $T_{test}=240^\circ\text{C}$ )

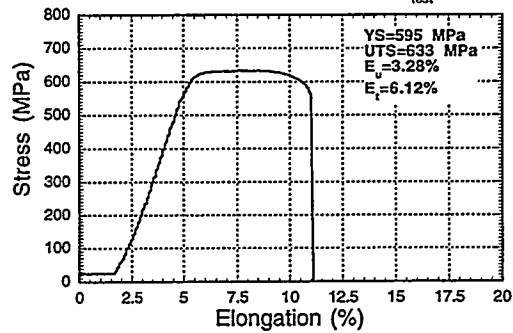


Fig. 8. Load-elongation curves for CuNiBe (heat #46546) longitudinal tensile specimens irradiated at 110 and 240°C.

## Discussion

One useful parameter for evaluating the suitability of a material for high-heat flux structural applications is the thermal stress figure of merit,  $M = \sigma_y k_{th} (1 - \nu) / \alpha E$ . This parameter can be calculated for the two Hycon 3HP™ CuNiBe heats from the present data by assuming that the temperature-dependent pure copper values [1] for Young's modulus ( $E$ ), Poisson's ratio ( $\nu$ ) and the coefficient of thermal expansion ( $\alpha$ ) are also valid for the alloy, and by utilizing the Wiedemann-Franz relation to convert the electrical conductivity measurements to thermal conductivity ( $k_{th}$ ). The calculated values at room temperature are  $M=60$  and  $57$  kW/m for heats 33667 and 46546 (longitudinal orientations), respectively. These values are significantly higher than the thermal stress figure of merit of other high-strength, high-conductivity copper alloys. For example, the calculated room temperature values for as-wrought GlidCop AL25 dispersion strengthened copper and cast & aged CuCrZr are  $M=39$  and  $37$ , respectively. The calculated thermal stress figure of merit decreases with increasing temperature for all of the copper alloys, mainly due to the decrease in yield strength (and also minor decreases in thermal conductivity and an increase in the Poisson's ratio which are partially balanced by a decrease in Young's modulus). The values at  $500^\circ\text{C}$  are  $M=36$  and  $34$  kW/m for CuNiBe heat #s 33667 and 46546, respectively. These values are about a factor of two larger than the calculated values at  $500^\circ\text{C}$  for GlidCop AL25 and CuCrZr of  $M=14$  and  $18$  kW/m, respectively.

The main disadvantage associated with CuNiBe alloys is poor ductility at elevated temperatures. The observed change in deformation mode from transgranular to intergranular failure with increasing test temperature is a common feature in FCC metals [15]. However, the physical mechanism responsible for the dramatic decrease in uniform elongation with increasing test temperature up to  $500^\circ\text{C}$  is not readily apparent from the TEM studies performed to date. Further work is needed to identify the cause of the low ductility in these two alloy heats at test temperatures above  $\sim 300^\circ\text{C}$ . It is worth noting that higher elongations (e.g., 5% at  $500^\circ\text{C}$ ) have been obtained in an AT temper of this alloy [16].

The observed radiation hardening and decrease in tensile elongation in the three CuNiBe specimens irradiated at  $110$ - $240^\circ\text{C}$  is qualitatively similar to the behavior observed in other high-strength, high-conductivity copper alloys [1-5,8]. It is worth noting that the reported uniform elongations of GlidCop AL25 and CuCrZr specimens irradiated in this temperature range are generally lower than the CuNiBe values. Figure 9 compiles the unirradiated and irradiated tensile data on Hycon 3HP™ CuNiBe (heat #46546) obtained at Risø [8] and ORNL. The data indicate that the radiation hardening component decreases with increasing irradiation temperature, and becomes negligible at temperatures above  $250$ - $300^\circ\text{C}$ . The elongation data indicate that radiation hardening at  $\sim 100^\circ\text{C}$  induces severe embrittlement ( $\epsilon_u < 1\%$ ), and that the tensile elongation increases rapidly between irradiation temperatures of  $200$  and  $\sim 250^\circ\text{C}$ . The irradiation datum obtained at  $350^\circ\text{C}$  suggests that the low ductility observed in CuNiBe at high temperatures prior to irradiation is maintained (or perhaps slightly more pronounced) following high temperature irradiation.

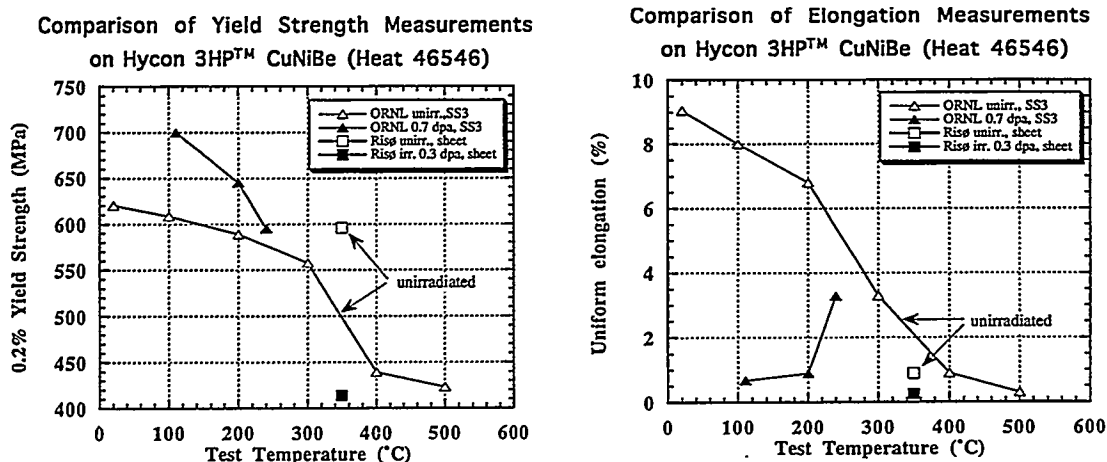


Fig. 9. Yield strength and elongation vs. temperature for unirradiated and irradiated Hycon 3HP™ CuNiBe.

### Acknowledgements

The two Hycon 3HP™ alloy heats for this study were supplied by David Krus, Brush-Wellman Inc. The authors thank L.L. Snead for experimental assistance with the HFBR neutron irradiation, and J.E. Pawel-Robertson for assistance with the irradiated tensile data acquisition.

### References

1. S.J. Zinkle and S.A. Fabritsiev, Nuclear Fusion (Atomic and Plasma-Material Interaction Data for Fusion supplement) 5 (1994) 163-192; also Fusion Materials Semiann. Prog. Report for period ending March 31, 1994, DOE/ER-0313/16, pp. 314-341.
2. S.A. Fabritsiev, S.J. Zinkle and B.N. Singh, "Evaluation of Copper Alloys for Fusion Reactor Divertor and First Wall Components," 7th Intern. Conf. on Fusion Reactor Materials, Obninsk, Russia, Sept. 1995, proceedings to be published in J. Nucl. Mater.
3. S.A. Fabritsiev, A.S. Pokrovsky, S.J. Zinkle and D.J. Edwards, "Low Temperature Embrittlement of Copper Alloys," 7th Intern. Conf. on Fusion Reactor Materials, Obninsk, Russia, proceedings to be published in J. Nucl. Mater.
4. S.A. Fabritsiev, A.S. Pokrovsky, S.J. Zinkle, A.F. Rowcliffe, D.J. Edwards, F.A. Garner, V.A. Sandakov, B.N. Singh and V.R. Barabash, "The Effect of Neutron Spectrum on The Mechanical and Physical Properties of Pure Copper and Copper Alloys," 7th Intern. Conf. on Fusion Reactor Materials, Obninsk, Russia, proceedings to be published in J. Nucl. Mater.
5. B.N. Singh, D.J. Edwards, A. Horsewell and P. Toft, Risø-R-839 (EN) Sept. 1995.
6. H.A. Murray, I.J. Zatz and J.O. Ratka, in Cyclic Deformation, Fracture, and Nondestructive Evaluation of Advanced Materials, 2nd Vol., ASTM STP 1184, M.R. Mitchell and O. Buck, eds. (ASTM, Philadelphia, 1994) pp. 109-133.
7. J.O. Ratka and W.D. Spiegelberg, IEEE Trans. Mag. 30, No. 4 (July 1994) 1859.
8. B.N. Singh, Risø National Laboratory, viewgraphs presented at ITER Working Group Meetings on Irradiation Testing of In-Vessel Structural Materials and Components (Gatlinburg, Tennessee, Nov. 5-10, 1995) and Materials and Joints for In-Vessel Components (Garching, Germany, May 13-16, 1996).
9. H. Murray, I.D. Harris and J.O. Ratka, Proc. 14th IEEE/NPSS Symp. on Fusion Engineering (1991) p. 272; H. Murray, *ibid.* p. 280.
10. J.C. Harkness, W.D. Spiegelberg and W.R. Cribb, Metals Handbook, 10th Ed., Vol. 2 (ASM International, 1990) p. 403.
11. D.J. Alexander, L.L. Snead, S.J. Zinkle, A.N. Gubbi, A.F. Rowcliffe and E.E. Bloom, "Effects of Irradiation at Low Temperature on V-4Cr-4Ti," in Fusion Materials Semiann. Prog. Report for period ending June 30, 1996, DOE/ER-0313/20, this report.
12. A. Guha, in High Conductivity Copper and Aluminum Alloys, eds. E. Ling and P.W. Taubenblat (TMS/AIME, Warrendale, PA, 1984) p. 133.
13. J.A. Spitznagel et al., Nucl. Instr. Meth. B 16 (1986) 279.
14. R.J. Rioja and D.E. Laughlin, Acta Metall. 28 (1980) 1301.
15. H.W. Hayden, W.G. Moffatt and J. Wulff, The Structure and Properties of Materials, Vol. III: Mechanical Behavior (Wiley & Sons, New York, 1965), p. 122.